Hydrogen storage capacity in single-walled carbon nanotubes

Yuchen Ma,[1] Yueyuan Xia,[2,*] Mingwen Zhao,[2] and Minju Ying[1]
[1]*Department of Optoelectronics and Information Engineering, Shandong University, Jinan, Shandong 250100, People's Republic of China*
[2]*Department of Physics, Shandong University, Jinan, Shandong 250100, People's Republic of China*
(Received 17 January 2002; published 11 April 2002)

Molecular-dynamics simulations were used to investigate the storage capacity of hydrogen in single-walled carbon nanotubes (SWNT's) and the strain of nanotube under the interactions between the stored hydrogen molecules and the SWNT. The storage capacities inside SWNT's increase with the increase of tube diameters. For a SWNT with diameter less than 20 Å, the storage capacity depends strongly on the helicity of a the SWNT. The maximal radial strain of SWNT is in the range of 11%–18%, and depends on the helicity of the SWNT. The maximal strain of armchair SWNT's is less than that of zigzag SWNT's. The tensile strengths of SWNT's decrease with increasing diameters, and approach that of graphite (20 GPa) for larger-diameter tubes.

DOI: 10.1103/PhysRevB.65.155430 PACS number(s): 61.46.+w, 81.07.De, 84.60.Ve

I. INTRODUCTION

Carbon nanotubes are formed by the seamless rolling of one or several graphite sheets over themselves. Being an example of low-dimensional nanostructures with inner hollow cavities, carbon nanotubes have attracted much theoretical and experimental interests. Carbon nanotubes have excellent mechanical, optical, electronical properties, etc., which depend on the helicities and diameters of nanotubes. The inner hollow cavity of a nanotube can serve as storage media for atoms and small molecules and nanometer-scale capsules for chemical reactions.[1–8] A carbon nanotube has good capillarity and can draw liquid and gas inside the nanotubes or the interstices between nanotubes.[1,2] As a future pollution-free energy source, the storage of hydrogen in carbon nanotubes has been studied extensively.[1–8] In fact, single-walled carbon nanotubes (SWNT's) with diameters of the order of 1 nm have been proposed as one of the possible candidates to approach the pursued level of packing.[2] From a fundamental point of view, the strong confinement of particles inside a SWNT offers the possibility of an experimental realization of a quasi-one-dimensional system.[5] Carbon nanotubes can withstand high stress in both axial and radial directions.[9,10] The excellent mechanical properties make carbon nanotubes able to accommodate very high-density materials.[3,4]

Most of the theoretical work on the hydrogen storage in SWNT's tried to find the optimal geometry of SWNT arrays, including diameters of SWNT's, distances between the nearest-neighbor nanotubes, and the relative arrangement of nanotubes, so that the volumetric density and weight efficiency of stored hydrogen can meet the goals of the DOE (Department of Energy) hydrogen plan (62 H_2 kg m^{-3} and 6.5 wt. %, respectively) for fuel cell powered vehicles.[6,7,11] Ambient temperature and pressure were also considered. Lee and Lee[3] performed density-functional and density-functional-based tight-binding calculations to predict the storage capacity in a SWNT. They claimed that the hydrogen storage capacity increased linearly with the diameters of SWNT's. The relation between the storage capacity and the type of a SWNT, including the diameter and helicity, are far from being clearly understood. The mechanical properties of the tube determine the storage capacity. For SWNT's of different diameters and helicities, the mechanical properties are different.[12]

The usual way to draw materials into nanotubes is by capillarity through the open ends of tubes,[1,2,6–8], and the materials inside the tubes will reach an equilibrium with the environments. The deformation of the nanotube, mainly in the radial direction, is expected to be very little, and till now no experimental work has been done to investigate such effect. Theoretical studies usually assumed that carbon nanotubes are rigid.[6–8] The excellent mechanical properties of carbon nanotube have not been used in the storage of materials. To do so, a way different from the conventional capillarity method should be used. Atoms can also be inserted into nanotubes by conventional implantation technique.[4,13,14] The ends of the SWNT must be closed to prevent the leakage of encapsulated atoms during the implantation process, because the atoms still have some kinetic energy after entering the tube. Comparing with the ends of tubes, the walls of tubes have much more surface area. The efficiency of the implantation through the wall will be much higher than that through the closed ends. So in our simulations, hydrogen atoms are all implanted through the sidewall of the SWNT. Experiments in this respect have been performed,[15,16] where the walls of carbon nanotubes were irradiated by Ar ion beams. However, the purposes of these experiments were to study nanotube amorphization and formation of defects, and so the incident energy of the Ar ion beam was very high (hundreds to thousands eV). Experiments in the low incident energy range, just as the energy used in our simulations, have not been reported yet.

In this paper we used molecular-dynamics simulation method to investigate the storage properties of a SWNT. We have proved that with appropriate initial kinetic energy, hydrogen atom can enter the tube without leaving defects on the tube wall.[4,13] Hydrogen atoms were consecutively implanted into the closed SWNT through the hexagonal ring on the tube wall at the incident energy of 20 eV. Hydrogen atoms inside the closed SWNT could form H_2 molecules via collisional reaction. The closure of the SWNT prevents H_2 molecules from escaping from its open ends.

II. SIMULATION METHODS

For our calculations, we used a realistic many-body Tersoff-Brenner potential[17,18] to model the interatomic forces between hydrogen and carbon atoms, among carbon atoms, and among hydrogen atoms. The potential has been used to describe diamond, graphite, carbon nanotubes, and many hydrocarbon complexes, and the results are in agreement with those obtained from experiments and quantum chemical calculations. This potential was also splined to a hard-core potential of Biersack-Ziegler type[19] to take into account the close-distance collisions. The long-distance van der Waals forces among H_2 molecules and between the SWNT and the H_2 molecules were described by the 6-12 Lennard-Jones-type interaction potential. The van der Waals parameters for the interaction between carbon and hydrogen were obtained from Ref. 20 and those for the interactions between H_2 molecules from Ref. 21. The intermolecular van der Waals potential between H_2 molecules is spherical and independent of the orientation of the H_2 molecules. The temperature of the system under study could be changed if necessary, by using a Langevin molecular-dynamic scheme,[22] which combines simulated annealing with molecular-dynamics simulation. During the implantation processes, the temperature of the H-tube system was kept at room temperature.

Calculations were performed for the following tubes: (5,5), (9,0), and (10,10) SWNT's. Every end of the (5,5) and (9,0) tubes was capped by a hemisphere of a C_{60} molecule, and the (10,10) tube by a hemisphere of a C_{240} molecule, as shown in Fig. 1. The (5,5), (9,0), and (10,10) capsules consist of 210, 222, and 540 carbon atoms, respectively. The radii of the fully relaxed (5,5), (9,0), and (10,10) SWNT's are 3.43 Å, 3.57 Å, and 6.79 Å, respectively. Farajian *et al.*[14] proved that the impact waves induced by the collisions of Na and K atoms with the wall of a SWNT at high incident energy (70 eV for Na and 150 eV for K) propagate only a short distance, roughly equal to the length of two hexagons, along the axial direction of the SWNT. We also tried longer SWNT's, but the results are same. So the given SWNT's were long enough so that the capped ends have neglect effects on the middle parts of the tubes and the middle parts could represent infinite long tubes.

III. RESULTS AND DISCUSSION

The interaction between the SWNT and H_2 molecule comes mainly from the intermolecular van der Waals forces. Due to the small diameters of the (5,5) and (9,0) tubes, the interaction energies have minimal values when the H_2 molecule locates at the axes of these tubes. But the minimal value is at the position 2.96 Å away from the tube wall for the (10,10) tube, the same as the interaction between H_2 molecule and graphite.[23] So H_2 molecules first coat the (10,10) tube's inner wall, but first populate at the axes of the (5,5) and (9,0) tube. With the increase of implanted hydrogen atoms, more H_2 molecules are formed inside the tubes. The van der Waals interactions between H_2 molecules make them distribute uniformly. The repulsive forces exerted on the tube wall by the H_2 molecules make the tube expand accordingly.

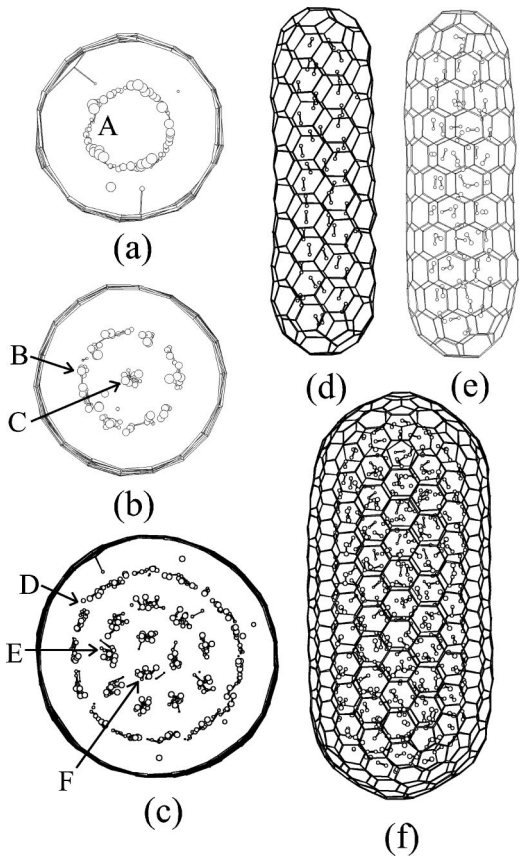

FIG. 1. Top views and side views of the H-SWNT complexes at the maximal hydrogen storage capacities for three different SWNT's. (a) and (d) for (5,5) SWNT; (b) and (e) for (9,0) SWNT; (c) and (f) for (10,10) SWNT. *A*,*B*,*D*,*E*,*F* denote the cylindrical shells formed by H_2 molecules and *C* denotes the axial phase. Hollow circles represent hydrogen atoms.

When the repulsive interactions exceed what the SWNT's can withstand, the tube wall will break. We found that the defined (5,5), (9,0), and (10,10) capsules can accommodate at most 43, 61 and 267 H_2 molecules, respectively. The corresponding volumetric densities are 142 kg/m^3, 172 kg/m^3 and 177 kg/m^3 for the (5,5), (9,0), and (10,10) tubes respectively. The corresponding weight efficiencies are about 3.5 wt. %, 5.0 wt. %, and 9.1 wt. %, respectively (the carbon atoms and hydrogen atoms around the ends are excluded while calculating the weight efficiency). The structures of the H-SWNT complexes at these densities are shown in Fig. 1. All the complexes have been fully relaxed. Figures 1(a) and 1(d) are for the (5,5) tube, 1(b) and 1(e) for the (9,0) tube, and 1(c) and 1(f) for (10,10) tube. Figures 1(a)–1(c) are the top views after cutting the atoms around the ends for clarity. Figures 1(d)–1(f) are the side views. Besides H_2 molecules, there are some free single hydrogen atoms and some hydrogen atoms chemisorbed on the wall.[4] H_2 molecules account for 95%. As seen from Fig. 1, the stored H_2 molecules can form a cylindrical lattice (shell-localized phase), and an axial phase in the tube.[24] In the (5,5) SWNT, only shell phase can be found. In (9,0) SWNT, both shell phase and axial phase emerge.

The interaction between the enclosed H_2 molecules and

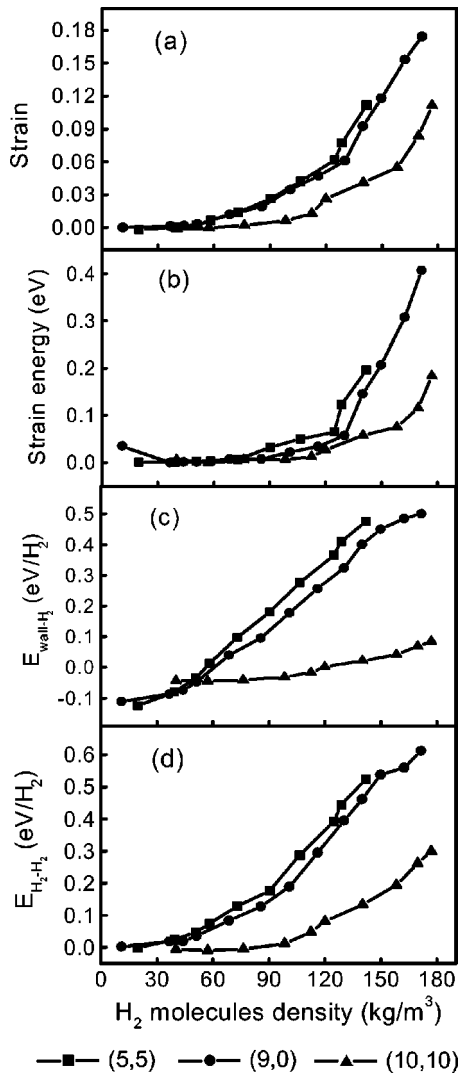

FIG. 2. The strains (a) and the strain energies (b) of the SWNT's, the interaction energies ($E_{wall\text{-}H_2}$) between the SWNT's and the stored H_2 molecules (c), and the interaction energies ($E_{H_2\text{-}H_2}$) between the stored H_2 molecules (d), as a function of the stored H_2 molecules densities for the (5,5), (9,0), and (10,10) SWNT's.

the tube wall induces the strain ($\Delta r/r_0$) of the tube in the radial direction, where r is the radius of the SWNT and r_0 is the original radius of the SWNT before implantation. The strains and the strain energies ($\Delta E_{wall}/n_C$) of the three SWNT's are shown in Figs. 2(a) and 2(b), respectively, as a function of the H_2 molecules density, where ΔE_{wall} is the energy gain of the wall of the nanotube with strain $\Delta r/r_0$ relative to the wall of the original nanotube before implantation, and n_C is the number of carbon atoms on the wall. The maximal strains of the (5,5) and the (10,10) tubes are nearly the same, 11%, while the (9,0) tube can sustain much higher strain, 18%. The maximal strain energy of the (9,0) tube is nearly two times those of the (5,5) and the (10,10) tubes. It is evident that the strain depends on the helicity. So although the (5,5) and the (9,0) SWNT's have nearly the same original radii, the maximal radii will be different, 3.80 Å and 4.20 Å for the (5,5) and (9,0) SWNT's, respectively. The (9,0) SWNT can provide more space and so may accommodate more H_2 molecules than the (5,5) SWNT. This can explain why in the (5,5) SWNT only shell phase emerges but both shell phase and axial phase are formed in the (9,0) SWNT. The radial expansion of the (5,5) SWNT comes mainly from the elongation of the bonds on the wall, which are perpendicular to the axis of the tube. The number of such bonds in an armchair ring on the wall is ten. However the radial expansion of the (9,0) SWNT comes mainly from the elongation of the bonds on the wall which have angles of about 60° to the axis of the tube. The number of such bonds in a zigzag ring on the wall is 18. Under the maximal strains, the lengths of these bonds approach the threshold, above which the bonds will break. According to this, we can estimate the ratio of the maximal strain of the (5,5) SWNT to that of the (9,0) SWNT to be 10/18, approximate to the simulation results of 11/18. This can explain why the armchair nonotubes are brittler than the zigzag nanotubes. As seen from both figures in Fig. 2, the curves have several turning points for the three SWNT's. After each turning point, the strains and the strain energies increase more rapidly with respect to the H_2 molecules density. This phenomenon is attributed to the change of the arrangement of H_2 molecules in the tube, such as the formation of new shells or the axial phase.

The interaction energies between the tube wall and H_2 molecules ($E_{wall\text{-}H_2}$) and those among the H_2 molecules ($E_{H_2\text{-}H_2}$) come mainly from the intermolecular van der Waals energy. Figures 2(c) and 2(d) show the interaction energies $E_{wall\text{-}H_2}$ and $E_{H_2\text{-}H_2}$ as a function of the H_2 molecules density. $E_{wall\text{-}H_2}$ is calculated by

$$E_{wall\text{-}H_2}=[E_t(\mathrm{SWNT+H})-E_t(\mathrm{SWNT})-E_t(\mathrm{H})]/n_{H_2}, \tag{1}$$

and similarly $E_{H_2\text{-}H_2}$ is calculated by

$$E_{H_2\text{-}H_2}=[E_t(\mathrm{H})-n_{H_2}E_{H_2}]/n_{H_2}, \tag{2}$$

where E_t(SWNT+H) and E_t(SWNT) are the total energies of the SWNT with and without hydrogen inside, respectively. E_t(H) is the total energy of hydrogen in the SWNT, n_{H_2} and E_{H_2} are the number of H_2 molecules and the energy of a single H_2 molecule, respectively. $E_{wall\text{-}H_2}$ of the (10,10) SWNT changes much less than those of the (5,5) and the (9,0) tubes. For the (10,10) tube, $E_{wall\text{-}H_2}$ has a minimal value of -44 meV at the density of 57 kg/m^3. The absolute value is close to the isosteric heat of adsorption of a complete monolayer of H_2 adsorbed on plana graphite (4 kJ/mol).[23] At this density, $E_{H_2\text{-}H_2}$ also has a minimum of -90 meV in the (10,10) tube. The H_2 molecules form a cylindrical shell with the distance of 2.95 Å to the tube wall. The shell density (n_i/S_i) is about 0.087 H_2 Å^{-2} and is within the experimentally observed density range of hydrogen molecules physisorbed on graphite,[25] where n_i is the number of H_2 molecules on the ith cylindrical shell and S_i is the surface area of this shell. So we predicted that H_2 molecules can even exist stably in open-ended (10,10) SWNT at

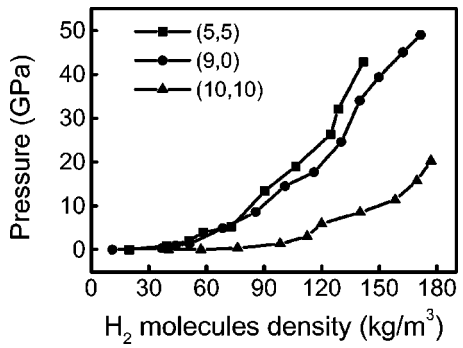

FIG. 3. The pressure imposed on the inner walls of the SWNT's as a function of the stored H_2 molecules densities for the (5,5), (9,0), and (10,10) SWNT's.

this density if there are no external perturbations. The (10,10) SWNT has exhibited some properties of graphite. The average distances between the nearest-neighbor H_2 molecules at the maximal storage densities in the (5,5), (9,0), and (10,10) tubes are 2.29, 2.29, and 2.42 Å, respectively.

The H_2 molecules inside the SWNT impose pressure on the inner surface of the tube. If the pressure exceeds the tensile strength of the tube, the tube will rupture and the H_2 molecules will leak out. From the pressure, we can get the tensile strength of the SWNT. Figure 3 shows the pressure for the three tubes as a function of the stored H_2 molecules density. We consider the pressure at RT (300 K). The pressure can be divided into two different components. The first is called the static pressure, and represents the repulsive force exerted on the inner wall of the tube by the H_2 molecules inside the tube. The second is the dynamic pressure, which stems from the momentum transfer to the inner wall of the tube caused by the thermal motion of the H_2 molecules at RT. We have evaluated these pressures, and the pressure values given in this paper are the sum of these two kinds. The maximal pressures that the (5,5) and the (9,0) tubes can withstand are 43 GPa and 49 GPa, respectively. Considering the statistical error, they can be regarded as the same. The helicity has little effect on the tensile strength. The maximal pressure that the (10,10) SWNT can withstand is only half of them, 20 GPa; the same as the in-plane tensile strength of graphite (20 GPa).[26] The tensile strength of the SWNT depends on the diameter. We predicted that for SWNT's with diameters in the range of 7.0–14.0 Å, the tensile strength is in the range of 20–50 GPa. For SWNT's with diameters larger than 14.0 Å, the tensile strength will be around 20 GPa, the same as graphite. This tensile strength range is within the values obtained by Yu *et al.*,[9] who measured the average breaking strength of 15 SWNT's experimentally and gave the range from 13 to 52 GPa. Considering that the (10,10) SWNT has more space inside, although the tensile strength of the (10,10) SWNT is only half of those of the (5,5) and (9,0) SWNT's, the storage capacities of the (10,10) tube, including volumetric density and weight efficiency, are not less than those of the (5,5) and (9,0) tubes.

In Fig. 1, A,B,D,E, and F denote the cylindrical shells and C denotes the axial phase. The shell densities of shells A,B,D,E, and F are about 0.18, 0.18, 0.16, 0.16, and 0.16 H_2 Å^{-2}, respectively. The linear density of the axial phase C is about 0.44 H_2 Å^{-1}. The distance between shell B to the axis C (d_{B-C}) is 2.15 Å. The distances between shells D and E (d_{D-E}), between E and F (d_{E-F}) are both about 2.0 Å. The distance between shell D and the tube wall is 2.27 Å. The shell density of shell B in the (9,0) SWNT is larger than that in the (10,10) tube, but d_{B-C} is greater than d_{D-E} and d_{E-F}. Under the confinement of the tube in the axial direction, the shell density and the linear density cannot be much low, so the distances between adjacent shells cannot be much small. We predicted that for a larger-diameter SWNT (>14 Å), the shell density, the distance between adjacent shells, and the distance from the tube wall to the outest shell will be around 0.16 H_2 Å^{-2}, 2.0 Å, and 2.27 Å, respectively. The (9,0) and the (5,5) SWNT's have the minimal (0°) and the maximal (30°) helical angles, respectively. The maximal strain of the SWNT with other helicity (0°∼30°) will be between those of the (5,5) and (9,0) SWNT's (11%–18%). According to the above data, we can estimate the storage capacity of a SWNT with definite diameter and helicity. Figures 4(a) and 4(b) show the estimated storage capacities of other 11 SWNT's with diameters in the range of 7 Å–33 Å by the above assumption—five armchair SWNT's and six zigzag SWNT's. When the diameter is less than 20 Å, volumetric density depends on the helicity of the SWNT. With the increase of diameter, the effect of helicity diminishes gradually. The increase in volumetric density lessens with the increase of the diameter. For both armchair and zigzag SWNT's, weight efficiency increases nearly linearly in this diameter range. The weight efficiencies of the zigzag SWNT's is always larger than those of the armchair SWNT's with same diameters.

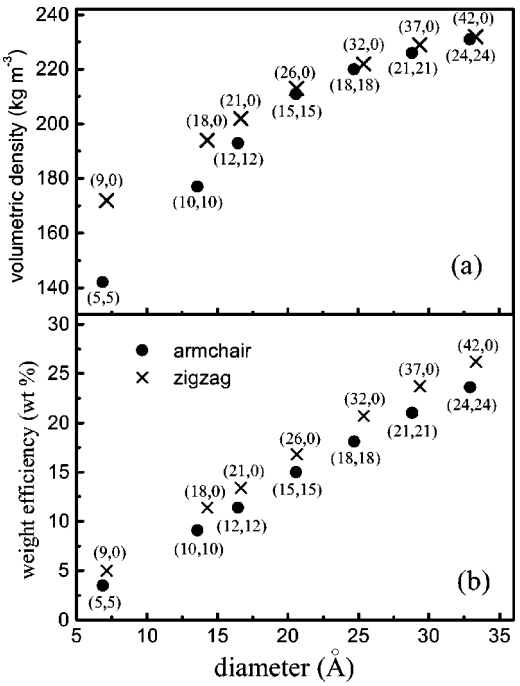

FIG. 4. The storage capacities of H_2 molecules in 14 SWNT's with different diameters and helicities. (a) volumetric density, (b) weight efficiency.

It is interesting to compare our results with the experimental[1,2] and theoretical[6,7] results obtained by other scientists. In their work, H_2 molecules not only exist in the open-ended SWNT's, but are also adsorbed by the exterior surfaces of SWNT's and/or the interstitial spaces between bundled tubes. Ye *et al.*[1] have found that hydrogen adsorption could exceed 8 wt. % on the ropes of SWNT's with individual SWNT diameters of about 13 Å. Dillon *et al.*[2] also reported that crystalline SWNT's with individual SWNT diameter being ~ 12 Å had a capacity for hydrogen sorption of 5–10 wt. % at pressure less than 1 bar near RT and they also predicted that SWNT's with large diameters, such as (12,12) and (15,15) SWNT's, could meet the target of DOE's hydrogen plan if excess pressure was applied to overcome the H_2-H_2 repulsive interactions. The simulation performed by Williams and Eklund[7] showed that the adsorption capacity of H_2 on the outer surface and in the interior space of an individual (10,10) SWNT could reach 9.6 wt. %. These results are close to our results of 9.1 wt. % for the (10,10) tube. Theoretically, Darkrim and Levesque[6] predicted maximal hydrogen adsorption in SWNT's with a diameter of 22 Å and spacing of 11 Å equal to 11.24 wt. %, and the corresponding volumetric density reached is about 60 $\mathrm{kg\,m^{-3}}$. This diameter is close to those of (15,15) and (26,0) tubes used in our simulation. The volumetric densities and the weight efficiency are both less than ours, especially the volumetric density. Their results are encouraging. It will be a promising way to combine their method and our implantation method. First, hydrogen atoms are injected into individual capped SWNT's by the implantation method, then the SWNT's are collected to form crystalline ropes to adsorb more H_2 molecules on the exterior surfaces and the interstitial spaces between SWNT's. The DOE target may be met by this way. If this implantation method is for the application of a SWNT as a fuel cell, a way must be found to extract the hydrogen from the SWNT. The hydrogen extraction process needs to be studied in the furthur work. Lee *et al.*[27] have presented a flip-out mechanism for hydrogen extraction from the interior of a SWNT through the sidewall of the tube. Considering the advantage of stable and safe storage of superhigh volumetric density in SWNT's at RT, one may think about the potential for using this method in the field of storage of nuclear fusion fuel (deuterium and tritium). Therefore the high mechanical strength of SWNT's may find an application in hydrogen isotope containers under irradiation by super laser beams or super-high-energy heavy-ion beams for fusion studies.

IV. CONCLUSION

H_2 molecules could form cylindrical shell phase and axial phase in a SWNT. The storage capacity of H_2 molecules in a SWNT increases with the increase of the diameter of a SWNT. For SWNT's with diameters less than 20 Å, volumetric density of H_2 in SWNT's depends on the helicities of SWNT's, and the density in zigzag a SWNT is always larger than that in an armchair SWNT with about the same diameter. However, this dependency diminishes gradually with the increase of diameter. The storage weight efficiency of H_2 in zigzag SWNT's is always larger than that in armchair SWNT's with about the same diameter. The maximal radial strain of a SWNT ranges from 11% to 18%, depending on the helicity of the SWNT. The maximal strain of the armchair SWNT's is less than that of the zigzag SWNT. The tensile strengths of SWNT's decrease rapidly with the increase in their diameters, and approach that of graphite (20 GPa) when the diameter is 13.6 Å.

ACKNOWLEDGMENTS

This work was supported by the National Science Foundation of China under Grants Nos. 59972017 and 10175038, and by National Key Subjects of Fundamental Research Program.

*Corresponding author. FAX: 86-531-8565167. Email address: myc@sdu.edu.cn

[1] Y. Ye, C.C. Ahn, C. Witham, B. Fultz, J. Liu, A.G. Rinzler, D. Colbert, K.A. Smith, and R.E. Smalley, Appl. Phys. Lett. **74**, 2307 (1999).
[2] A.C. Dillon, K.M. Jones, T.A. Bekkedahl, C.H. Klang, D.S. Bethune, and M.J. Heben, Nature (London) **386**, 377 (1997).
[3] S.M. Lee and Y.H. Lee, Appl. Phys. Lett. **76**, 2877 (2000).
[4] Y.C. Ma, Y.Y. Xia, M.W. Zhao, R.J. Wang, and L.M. Mei, Phys. Rev. B **63**, 115422 (2001).
[5] M.C. Gordillo, J. Boronat, and J. Casulleras, Phys. Rev. Lett. **85**, 2348 (2000).
[6] F. Darkrim and D. Levesque, J. Phys. Chem. B **104**, 6773 (2000).
[7] K.A. Williams and P.C. Eklund, Chem. Phys. Lett. **320**, 352 (2000).
[8] M. Rzepka, P. Lamp, and M.A. de la Casa-Lillo, J. Phys. Chem. B **102**, 10 894 (1998).
[9] M.F. Yu, B.S. Files, S. Arepalli, and R.S. Ruoff, Phys. Rev. Lett. **84**, 5552 (2001).
[10] Z.W. Pan, S.S. Xie, L. Lu, B.H. Chang, L.F. Sun, W.Y. Zhou, G. Wang, and D.L. Zhang, Appl. Phys. Lett. **74**, 3152 (1999).
[11] F. Darkrim and D. Levesque, J. Chem. Phys. **109**, 4981 (1998).
[12] N. Yao and V. Lordi, J. Appl. Phys. **84**, 1939 (1998).
[13] Y.C. Ma, Y.Y. Xia, M.W. Zhao, M.J. Ying, X.D. Liu, and P.J. Liu, J. Chem. Phys. **115**, 8152 (2001).
[14] A.A. Farajian, K. Ohno, K. Esfarjani, Y. Marnyama, and Y. Kawazoe, J. Chem. Phys. **111**, 2164 (1999).
[15] Y. Zhu, T. Yi, B. Zheng, and L. Cao, Appl. Surf. Sci. **137**, 83 (1999).
[16] A.V. Krasheninnikov, K. Nordlund, M. Sirviö, E. Salonen, and J. Keinonen, Phys. Rev. B **63**, 245405 (2001).
[17] J. Tersoff, Phys. Rev. Lett. **61**, 2879 (1988).
[18] D.W. Brenner, Phys. Rev. B **42**, 9458 (1990).
[19] J.P. Biersack and J.F. Ziegler, Nucl. Instrum. Methods Phys. Res. **194**, 93 (1982).
[20] W.D. Cornell, P. Cieplak, C.I. Bayly, I.R. Gould, K.M. Merz, Jr., D.M. Ferguson, D.C. Spellmeyer, T. Fox, J.W. Caldwell, and P.A. Kollman, J. Am. Chem. Soc. **117**, 5179 (1995).
[21] I.F. Silvera and V.V. Goldman, J. Chem. Phys. **69**, 4209 (1978).
[22] R. Biswas and D.R. Hamann, Phys. Rev. B **34**, 895 (1986).
[23] E.L. Pace and A.R. Siebert, J. Phys. Chem. **63**, 1398 (1959).
[24] S.M. Gatica, M.W. Cole, G. Stan, J.M. Hartman, and V.H. Crespi, Phys. Rev. B **62**, 9989 (2000).

[25] H. Freimuth, H. Wiechert, H.P. Schildberg, and H.J. Lauter, Phys. Rev. B **42**, 587 (1990).
[26] H.O. Pierson, *Handbook of Carbon, Graphite, Diamond and Fullerenes: Properties, Processing and Applications* (Noyes, Park Ridge, NJ, 1993).
[27] S.M. Lee, K.H. An, Y.H. Lee, G. Seifert, and T. Frauenheim, J. Am. Chem. Soc. **123**, 5059 (2001).